Unsteady three-dimensional MHD flow and mass transfer in a porous space in the presence of thermal radiation

Olanrewaju, P. O.

Department of Mathematics, Covenant University, Ota, Nigeria, West Africa.

(oladapo_anu@yahoo.ie)

Abstract

Unsteady three-dimensional MHD flow and mass transfer in a porous is presented here by taking into account of thermal radiation. The governing fundamental equations are first transformed into system of ordinary differential equations using self similar transformation and they are solved numerically by using the sixth-order Runge-Kutta-Fehlberg method with shooting technique for some values of the physical parameters embedded in the flow model. Important features of the flow and heat transfer characteristic for different values of thermal radiation, magnetic field and chemical reaction are analyzed and discussed. Numerical results for the velocities, temperature and concentration profiles for a prescribed magnetic field, thermal radiation and chemical reaction parameters as well as the development of the local skin-friction coefficient, local Nusselt number and Sherwood number are reported graphically for various parametric conditions to show interesting aspect of the numerical solution.

Keywords: Unsteady flow: Three-dimensional stretching: Mass transfer: Porous medium: Radiation: Magnetic field.

1. Introduction

Boundary layer flow induced by a stretching surface has been studied extensively under varied conditions by many researchers because of its considerable engineering applications. For instance, aerodynamic extrusion of plastic sheets, cooling of metallic sheets in a cooling bath, in paper industry is few examples of such applications. Particularly, momentum and heat transfer in stretching flow of a viscoelastic fluid have been analyzed due to its ever increasing usage in manufacturing process of artificial film and artificial fibers. Literature survey establishes serious attention has been given to the steady two-dimensional flow bounded by a stretching surface whose velocity to the distance from a fixed origin varies linearly and non-linearly. Some recent contributions on the topic have been presented (see [1-10]). Recently, Xu et al. [11] looked at the unsteady three-dimensional magnetohydrodynamic (MHD) boundary layer flow and heat transfer over a stretching sheet. They have presented the series solutions for the mathematical problems. Very recently, Hayat et al. [12] studied homotopy solution for the unsteady three-dimensional MHD flow and mass transfer in a porous space.

Radiative heat transfer flow is very important in manufacturing industries for the design of reliable equipments, nuclear plants, gas turbines and various propulsion devices for aircraft, missiles, satellites and space vehicles. Similarly, the effects of thermal radiation on the forced and free convection flows are important in the content of space technology and processes involving high temperature. Based on these applications, England and Emery [13] studied the thermal radiation effect of an optically thin gray

gas bounded by a stationary vertical plate. Plumb et al [14] was the first to examine the effect of horizontal cross-flow and radiation on natural convection from vertical heated surface in saturated porous media. Rosseland diffusion approximation had been utilized in this investigation of convection flow with radiation. Makinde et al. [15] examined unsteady convection with chemical reaction and radiative heat transfer past a flat porous plate moving through a binary mixture. Makinde and Olanrewaju [16] studied unsteady mixed convection with Soret and Dufour effects past a porous plate moving through a binary mixture of chemically reacting fluid. Hayat et al. [17] investigated the effect of thermal radiation on the flow of a second grade fluid and the references there in. Similarly, very recently, Hayat et al. [d] studied effects of radiation and magnetic field on mixed convection stagnation-point flow over a vertical stretching sheet in a porous medium. Hayat et al. [18] examined the effects of radiation and magnetic field on the mixed convection stagnation-point flow over a vertical stretching sheet in a porous medium.

The aim of present work is to extend the analysis of Hayat et al. [12]] in three directions. To the best of author's knowledge, it has not been considered. Firstly, to examine the boundary layer flow in porous space. Secondly, to analyze the heat transfer effects. Thirdly, to describe the influence of mass transfer. Fourthly, to describe the effects of the embedded flow parameters that governs the flow model. Keeping this in view, we present the problems formulation in Section 2. Section 3 includes the method of solutions. In Section 4, the solutions are analyzed by various parameters. Finally, main observations are presented in Section 5.

2. Mathematical formulation

We consider the transient and three-dimensional flow of a viscous fluid over a stretching surface. The fluid is electrically conducting in the presence of a constant applied magnetic field B_0 and thermal radiation. The induced magnetic field is neglected under the assumption of a small magnetic Reynolds number. Initially (for t = 0), both fluid and plate are stationary and they have constant temperature T_∞ and Concentration C_∞. The plate at t = 0 is expressed by the velocity components u ax, v = by (u and v are the velocity components in x- and y-directions). Now, for this time the surface temperature and concentration vary from T_∞ to T_w and C_∞ to C_w, respectively. The mathematical statements for the boundary layer problems are

$$\frac{\partial u}{\partial x}+\frac{\partial v}{\partial y}+\frac{\partial w}{\partial z}=0, \tag{1}$$

$$\frac{\partial u}{\partial t}+u\frac{\partial u}{\partial x}+v\frac{\partial u}{\partial y}+w\frac{\partial u}{\partial z}=\upsilon\frac{\partial^2 u}{\partial z^2}-\frac{\sigma B_0^2}{\rho}u-\frac{\upsilon\varphi}{k}u, \tag{2}$$

$$\frac{\partial v}{\partial t}+u\frac{\partial v}{\partial x}+v\frac{\partial v}{\partial y}+w\frac{\partial v}{\partial z}=\upsilon\frac{\partial^2 v}{\partial z^2}-\frac{\sigma B_0^2}{\rho}v-\frac{\upsilon\varphi}{k}v, \tag{3}$$

$$\frac{\partial T}{\partial t}+u\frac{\partial T}{\partial x}+v\frac{\partial T}{\partial y}+w\frac{\partial T}{\partial z}=\alpha\frac{\partial^2 T}{\partial z^2}-\frac{\alpha}{k}\frac{\partial q_r}{\partial z}, \tag{4}$$

$$\frac{\partial C}{\partial t}+u\frac{\partial C}{\partial x}+v\frac{\partial C}{\partial y}+w\frac{\partial C}{\partial z}=D\frac{\partial^2 C}{\partial z^2}-k_1 C, \tag{5}$$

where w is the z-component of velocity, ρ is the fluid density, v is the kinematic viscosity, σ is the electrical conductivity, φ is the porosity, k is the permeability of the porous medium, C is the concentration species of the fluid, D is the diffusion coefficient of the diffusion species in the fluid, k_1 is the first-order homogeneous constant reaction rate and α is the thermal diffusivity.

The corresponding boundary conditions are

$$\begin{aligned} &u=v=w=0,\ \ T=T_\infty,\ \ \ C=C_\infty,\ \ t\prec 0,\\ &u=u_w=ax,\ \ v=v_w=by,\ w=0,\ T=T_w,\ \ C=C_w,\ \ z=0;\ \ t\geq 0,\\ &u\to 0,\ \ v\to 0,\ T\to 0,\ \ \ C\to 0,\ \ as\ \ \ z\to\infty;\ t\geq 0, \end{aligned} \tag{6}$$

Where the constants a and b are positive. The radiative heat flux q_r is described by Roseland approximation [10] such that

$$q_r = -\frac{4\sigma^*}{3K}\frac{\partial T^4}{\partial y}, \tag{7}$$

where σ^* and K are the Stefan-Boltzmann constant and the mean absorption coefficient, respectively. Following Chamkha [6], we assume that the temperature differences within the flow are sufficiently small so that the T^4 can be expressed as a linear function after using Taylor series to expand T^4 about the free stream temperature T_∞ and neglecting higher-order terms. This results in the following approximation:

$$T^4 \approx 4T_\infty^3 T - 3T_\infty^4. \tag{8}$$

Using (8) and (7) in (4), we obtain

$$\frac{\partial q_r}{\partial y} \approx -\frac{16\sigma^* T_\infty^3}{3K}\frac{\partial^2 T}{\partial y^2}. \tag{9}$$

Following Hayat et al. [12], it is convenient to use the following similarity transformations:

$$\begin{aligned} &\eta=\sqrt{\frac{a}{\upsilon\varepsilon}}z,\quad \varepsilon=1-\exp(-\tau),\ \ \tau=at,\ u=ax\frac{\partial f}{\partial\eta},\ v=ay\frac{\partial g}{\partial\eta},\ w=-\sqrt{a\upsilon\varepsilon}(f+g),\\ &\theta=\frac{T-T_\infty}{T_w-T_\infty},\qquad \phi=\frac{C-C_\infty}{C_w-C_\infty}. \end{aligned} \tag{10}$$

Eq. (1) is satisfied identically and Eqs. (2)-(5) becomes

$$f'''+(1-\varepsilon)\left(\frac{\eta}{2}f''-\varepsilon\frac{\partial f'}{\partial\varepsilon}\right)+\varepsilon\left[(f+g)f''-(f')^2-M^2f'-\lambda f'\right]=0, \tag{11}$$

$$g'''+(1-\varepsilon)\left(\frac{\eta}{2}g''-\varepsilon\frac{\partial g'}{\partial\varepsilon}\right)+\varepsilon\left[(f+g)g''-(g')^2-M^2g'-\lambda g'\right]=0, \tag{12}$$

$$\theta''\left[1+\frac{4}{3}Ra\right]+\Pr(1-\varepsilon)\left(\frac{\eta}{2}\theta'-\varepsilon\frac{\partial\theta}{\partial\varepsilon}\right)+\Pr\varepsilon(f+g)\theta'=0, \tag{13}$$

$$\phi''+Sc(1-\varepsilon)\left(\frac{\eta}{2}\phi'-\varepsilon\frac{\partial\phi}{\partial\varepsilon}\right)+Sc\varepsilon(f+g)\phi'-\gamma\,Sc\varepsilon\phi=0, \tag{14}$$

$$\begin{aligned} &f(\varepsilon,0)=g(\varepsilon,0)=0, f'(\varepsilon,0)=\theta(\varepsilon,0)=\phi(\varepsilon,0)=1, g'(\varepsilon,0)=c,\\ &f'(\varepsilon,\infty)=g'(\varepsilon,\infty)=\theta(\varepsilon,\infty)=\phi(\varepsilon,\infty)=0. \end{aligned} \tag{15}$$

Prime denotes the derivative with respect to η, c(= b/a) the stretching parameter is a positive constant. It was noted that when c = 0, the problem reduces to two-dimensional case. Here the local Hartman number M, the local porosity parameter λ, the Schmidt number Sc, the chemical reaction parameter γ and the thermal radiation parameter Ra are given by

$$M^2=\frac{\sigma B_0^2}{\rho a},\ \lambda=\frac{\upsilon\varphi}{ak},\ \mathrm{Pr}=\frac{\upsilon}{a},\ Sc=\frac{\upsilon}{D},\ \gamma=\frac{k_1}{a},\ Ra=\frac{4\alpha\sigma^* T_\infty^3}{K'k}. \tag{16}$$

Here, the skin friction coefficients C_{fx} and C_{fy} in x- and y-directions, local Nusselt number Nu and local Sherwood number Sh are

$$\begin{aligned}&\mathrm{Re}_x^{1/2}\,\varepsilon^{1/2}C_{fx}=-f''(\varepsilon,0),\quad \mathrm{Re}_y^{1/2}\,\varepsilon^{1/2}C_{fy}=-g''(\varepsilon,0),\\ &Nu\,\mathrm{Re}_x^{-1/2}\,\varepsilon^{1/2}=-\theta'(\varepsilon,0),\qquad Sh\,\mathrm{Re}_x^{-1/2}\,\varepsilon^{1/2}=-\phi'(\varepsilon,0),\end{aligned} \tag{17}$$

where $\mathrm{Re}_x = ax^2/\nu$ and $\mathrm{Re}_y = ay^2/\nu$ are the local Reynolds number, $f''(\varepsilon,0)\ and\ g''(\varepsilon,0)$ are the surface shear stresses in x- and y-directions, $\theta'(\varepsilon,0)$ is the surface heat transfer parameter and $\phi'(\varepsilon,0)$ is the surface mass transfer parameter.

For ε = 0, Eqs. (11)-(14) can be written as

$$\begin{aligned}&f'''+\frac{\eta}{2}f''=0,\\ &g'''+\frac{\eta}{2}g''=0,\\ &[1+\frac{4Ra}{3}]\theta''+\mathrm{Pr}\frac{\eta}{2}\theta'=0,\\ &\phi''+Sc\frac{\eta}{2}\phi'=0.\end{aligned} \tag{18}$$

Similarly for ε = 1, Eqs. (11)-(14) becomes

$$\begin{aligned}&f'''+(f+g)f''-f'^2-M^2f'-\lambda f'=0,\\ &g'''+(f+g)g''-g'^2-M^2g'-\lambda g'=0,\\ &[1+\frac{4Ra}{3}]\theta''+\mathrm{Pr}(f+g)\theta'=0,\\ &\phi''+Sc(f+g)\phi'-\gamma Sc\phi=0,\end{aligned} \tag{19}$$

subject to the boundary conditions (15).

3. Method of Solution

Here, we solve Eqs. (18) analytically and Eqs. (19) numerically using Shooting technique with sixth order of Runge-Kutta method. It can be seen that for ε = 0, Eq. (18) has a closed formed solution of the form

$$f(0,\eta)=\eta erfc\left(\frac{\eta}{2}\right)+\frac{2}{\sqrt{\pi}}\left[1-\exp\left(-\frac{\eta^2}{4}\right)\right],$$

$$g(0,\eta)=c\left(\eta erfc\left(\frac{\eta}{2}\right)+\frac{2}{\sqrt{\pi}}\left[1-\exp\left(-\frac{\eta^2}{4}\right)\right]\right),$$

$$\theta(0,\eta)=erfc\left(\frac{\left(\sqrt{\frac{3\,\mathrm{Pr}}{3+4Ra}}\right)}{2}\eta\right), \tag{20}$$

$$\phi(0,\eta)=erfc\left(\frac{\sqrt{Sc}}{2}\eta\right),$$

where

$$erfc(\eta)=1-\frac{2}{\sqrt{\pi}}\int_0^{\eta}\exp(-x^2)dx. \tag{21}$$

Eq. (19) constitutes a highly non-linear coupled boundary value problem of third and second-order. So we develop most effective numerical shooting technique with sixth-order Runge-Kutta integration algorithm. To select η_∞ we begin with some initial guess value and solve the problem with some particular set of parameters to obtain $f''(\varepsilon,0), g''(\varepsilon,0), \theta'(\varepsilon,0) and\ \phi'(\varepsilon,0)$. The solution process is repeated with another larger value of η_∞ until two successive values of $f''(\varepsilon,0), g''(\varepsilon,0), \theta'(\varepsilon,0) and\ \phi'(\varepsilon,0)$ differ only after desired digit signifying the limit of the boundary along η. The last value of η_∞ is chosen as appropriate value for that particular simultaneous equations of first order for seven unknowns following the method of superposition. To solve this system we require ten initial conditions whilst we have only two initial conditions. Now, we employ numerical shooting technique where these two ending boundary conditions are utilized to produce two unknown initial conditions at η = 0. In this calculation, the step size $\Delta\eta=0.001$ is used while obtaining the numerical solution with $\eta_{\max}=11$ and five-decimal accuracy as the criterion for convergence.

4. Results and discussion

Numerical calculations have been carried out for different values of the thermophysical parameters controlling the fluid dynamics in the flow regime. The values of Schmidt number (*Sc*) are chosen water vapour (*Sc* = 0.62), ammonia (*Sc* = 0.78) and Propyl Benzene (*Sc* = 2.62) at temperature 25^{o}C and one atmospheric pressure. The values of Prandtl number is chosen to be *Pr* = 0.72 which represents air at temperature 25^{o}C and one atmospheric pressure. In all computations we desire the variation of *f, g,* θ and ϕ versus η for the velocities, temperature and species diffusion boundary layers. Table (1) shows the computations for the influence of the embedded flow parameters on the local skin friction on x and y directions together with the heat and mass transfer rate at the moving plate surface. It is quite interesting to note that increase in Sc, and γ has no effects on the skin friction coefficients and the Nusselt number at the surface $f''(\varepsilon,0)$, $g''(\varepsilon,0)$ *and* $\theta'(\varepsilon,0)$ but increases the Sherwood number at the surface boundary layer. Skin friction coefficients at the surface increases as the Hartman number increases. It was also seen that the skin friction coefficients increases with an increase in the porosity parameter and at the same time decreasing the Nusselt and Sherwood number at the surface. Significantly, the radiation parameter Ra has appreciable influence on the heat transfer rate but with no effect on the other interesting physical quantities. It is noteworthy to note that the stretching parameter c has greater influence on the physical properties of the flow. It was seen clearly that increase in parameter c increases the skin friction coefficients, the Nusselt and Sherwood numbers at the surface boundary layer $f''(\varepsilon,0)$, $g''(\varepsilon,0), \theta'(\varepsilon,0)$ *and* $\phi'(\varepsilon,0)$. It is interesting to note that positive values of γ represent destructive and negative values represent generative chemical reaction. Increasing parameter γ increases the Sherwood number at the surface.

Table 1

Values of $f''(\varepsilon,0), g''(\varepsilon,0), \theta'(\varepsilon,0)\, and\ \phi'(\varepsilon,0)$ for the embedded flow parameters in the flow model when ε = 1.

M	*Sc*	*Pr*	*Ra*	*λ*	*γ*	*c*	$-f''(\varepsilon,0)$	$-g''(\varepsilon,0)$	$-\theta'(\varepsilon,0)$	$-\phi'(\varepsilon,0)$
0	**1**	**1**	**1**	**1**	**1**	**0.1**	**1.42707425**	**0.11989595**	**0.28417669**	**1.17092198**
0.1	**1**	**1**	**1**	**1**	**1**	**0.1**	**1.43056719**	**0.12031101**	**0.28378656**	**1.17074353**
0.3	**1**	**1**	**1**	**1**	**1**	**0.1**	**1.45821203**	**0.12358193**	**0.28074425**	**1.16934359**
0.4	**1**	**1**	**1**	**1**	**1**	**0.1**	**1.48198158**	**0.12637529**	**0.27819159**	**1.16815717**
0.1	**0.62**	**1**	**1**	**1**	**1**	**0.1**	**1.43056719**	**0.12031101**	**0.28378656**	**0.90796272**
0.1	**0.78**	**1**	**1**	**1**	**1**	**0.1**	**1.43056719**	**0.12031101**	**0.28378656**	**1.02595318**
0.1	**2.62**	**1**	**1**	**1**	**1**	**0.1**	**1.43056719**	**0.12031101**	**0.28378656**	**1.94693909**
0.1	**1**	**0.72**	**1**	**1**	**1**	**0.1**	**1.43056719**	**0.12031101**	**0.22732899**	**1.17074353**
0.1	**1**	**3.00**	**1**	**1**	**1**	**0.1**	**1.43056719**	**0.12031101**	**0.64411898**	**1.17074353**
0.1	**1**	**7.10**	**1**	**1**	**1**	**0.1**	**1.43056719**	**0.12031101**	**1.15093985**	**1.17074353**
0.1	**1**	**1**	**1**	**1**	**1**	**0.1**	**1.43056719**	**0.12031101**	**0.28378656**	**1.17074353**
0.1	**1**	**1**	**2**	**1**	**1**	**0.1**	**1.43056719**	**0.12031101**	**0.21079238**	**1.17074353**
0.1	**1**	**1**	**3**	**1**	**1**	**0.1**	**1.43056719**	**0.12031101**	**0.17818658**	**1.17074353**
0.1	**1**	**1**	**1**	**0.1**	**1**	**0.1**	**1.07235304**	**0.07445359**	**0.33135495**	**1.19109626**
0.1	**1**	**1**	**1**	**0.3**	**1**	**0.1**	**1.16132221**	**0.08668680**	**0.31800509**	**1.18562015**
0.1	**1**	**1**	**1**	**0.4**	**1**	**0.1**	**1.20341226**	**0.09222260**	**0.31206396**	**1.18313408**
0.1	**1**	**1**	**1**	**1**	**0.1**	**0.1**	**1.43056719**	**0.12031101**	**0.28378656**	**0.63711465**
0.1	**1**	**1**	**1**	**1**	**0.3**	**0.1**	**1.43056719**	**0.12031101**	**0.28378656**	**0.79351784**
0.1	**1**	**1**	**1**	**1**	**0.4**	**0.1**	**1.43056719**	**0.12031101**	**0.28378656**	**0.85919188**
0.1	**1**	**1**	**1**	**1**	**1**	**0.00**	**1.41774468**	**0.00000000**	**0.26665579**	**1.15485136**
0.1	**1**	**1**	**1**	**1**	**1**	**0.25**	**1.44945710**	**0.31642983**	**0.30811892**	**1.19400515**
0.1	**1**	**1**	**1**	**1**	**1**	**0.50**	**1.48012872**	**0.68163040**	**0.34556949**	**1.23142220**

A. Velocity Profiles

Figures 1-6 depict the effects of emerging flow parameters on non-dimensional velocity profiles. In figure 1 the effect of increasing the Hartman number on the momentum boundary-layer thickness is illustrated. Increasing this parameter lead to a decrease in the velocity which confirmed with the fact that the magnetic field presents a damping effect on the velocity by creating a drag force that opposes the fluid motion. Figure 2 shows a decrease in the fluid velocity within the boundary layer due to porosity parameter. This indicates the usual fact that porosity stabilizes the boundary layer growth. Furthermore, figures 3 show that an increase in the stretching parameter lead to a small decrease in the velocity profile. Figure 4-6 has similar effect with figures 1-3.

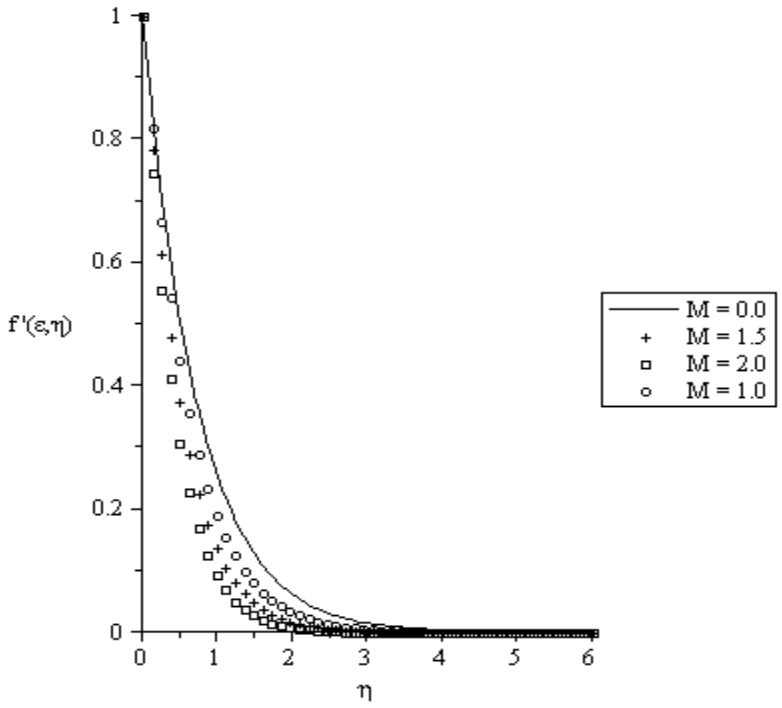

Figure 1: Velocity profiles for Ra = 1, Sc = 1, c = 0.5, ε = 1, λ = 0.5, Pr = 1, γ = 1.

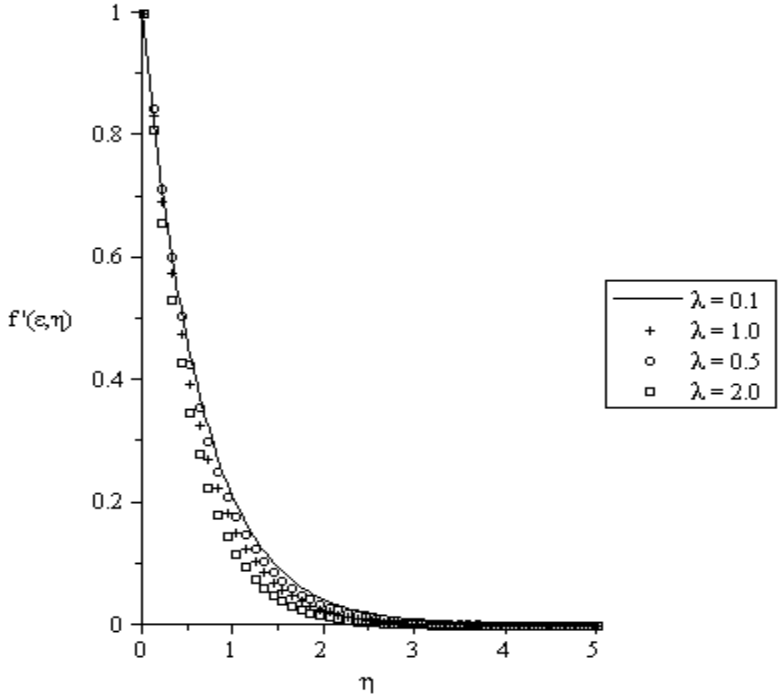

Figure 2: Velocity profiles for Pr = 1, M = 1, c = 0.5, ε = 1, Ra = 0.5, Sc = 1, γ = 1.

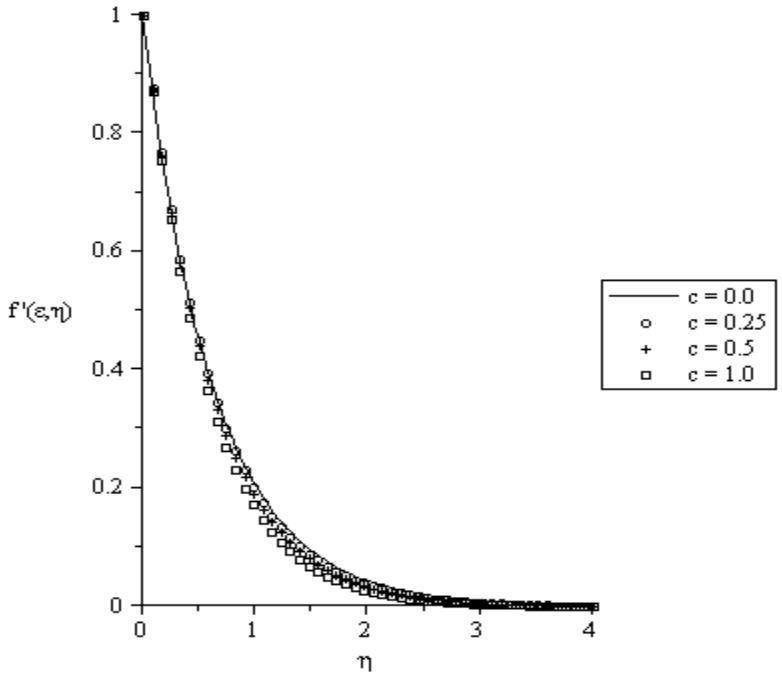

Figure 3: Velocity profiles for Pr = 1, M = 1, γ = 0.5, ε = 1, Ra = 0.5, Sc = 1, λ = 1.

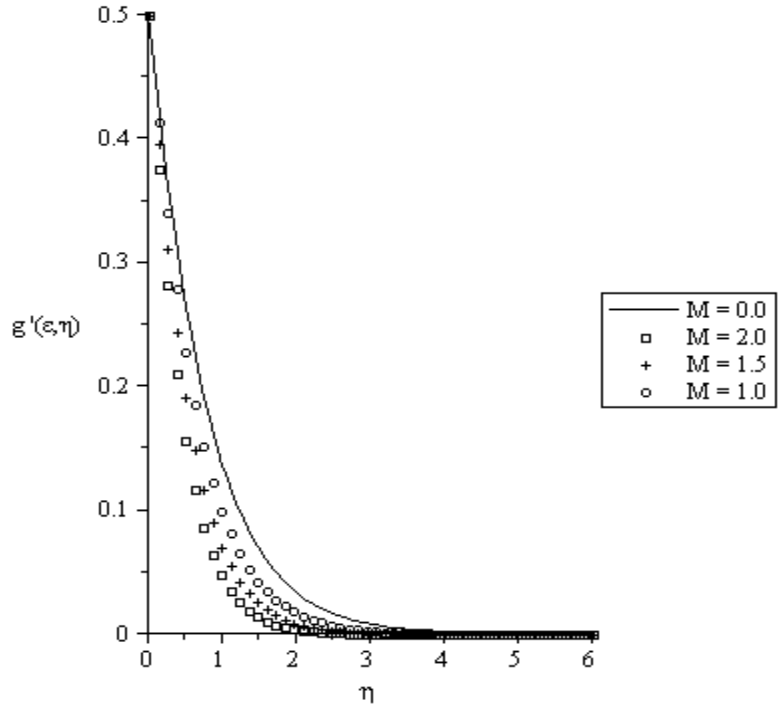

Figure 4: Velocity profiles for Ra = 1, Sc = 1, c = 0.5, ε = 1, λ = 0.5, Pr = 1, γ = 1.

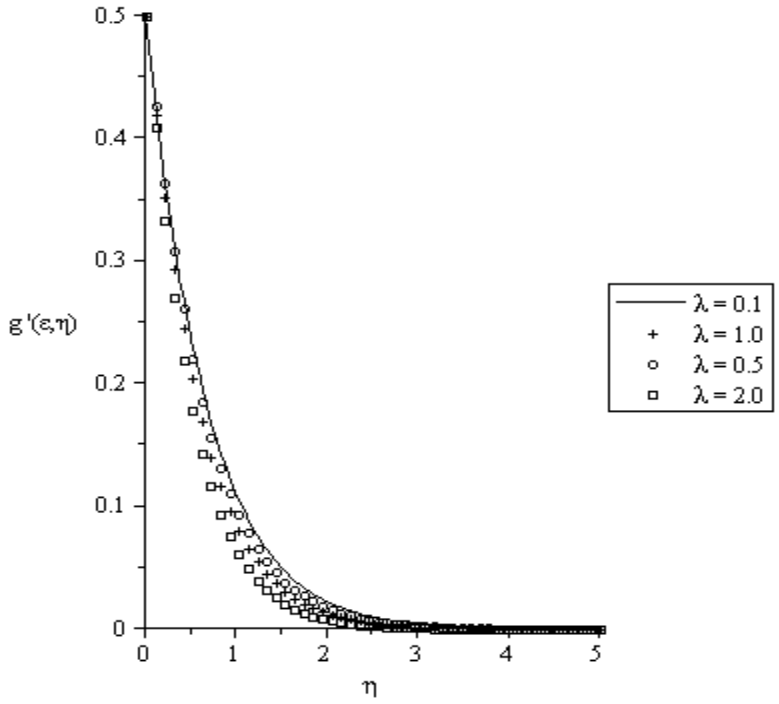

Figure 5: Velocity profiles for Pr = 1, M = 1, c = 0.5, ε = 1, Ra = 0.5, Sc = 1, γ = 1.

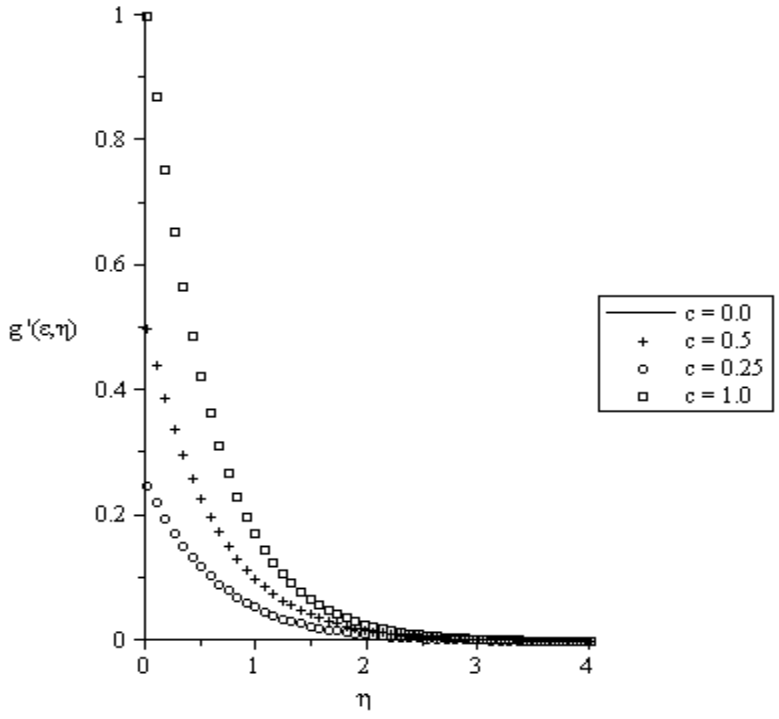

Figure 6: Velocity profiles for Pr = 1, M = 1, γ = 0.5, ε = 1, Ra = 0.5, Sc = 1, λ = 1.

B. Temperature Profiles

The effects of various thermophysical parameters on the fluid temperature are illustrated in Figures. 7 to 11. In figures 7, we observed that an increase in the Hartman number brings an increase in the thermal boundary layer thickness. Figure 8 shows the influence of Prandtl number on fluid temperature. It was seen that increase in the Prandtl number is to decrease the thermal boundary layer thickness across the plate. Figure 9 depicts the graph of temperature against spanwise coordinate η for various values of radiation parameter. Due to radiation absorption the thermal boundary layer thickness increases as the radiation parameter increases. It is interesting to note that increase in the porosity parameter increases the temperature boundary layer thickness (see figure 10). Figure 11 represents the temperature solution for various values of the stretching parameter c. It was noticed that the thermal boundary layer thickness decreases as the stretching parameter c increases across the plate.

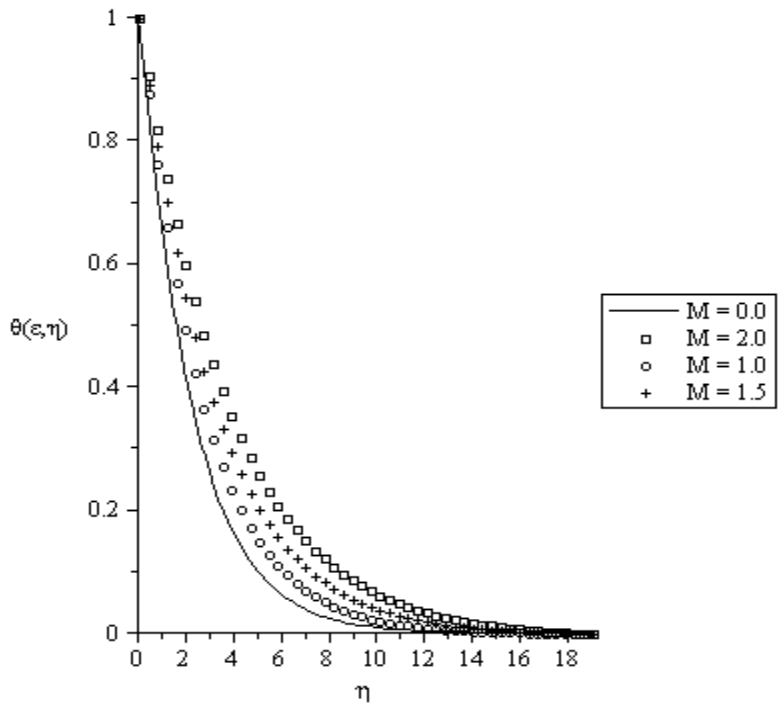

Figure 7: Temperature profiles for Ra = 1, Sc = 1, c = 0.5, ε = 1, λ = 0.5, Pr = 1, γ = 1.

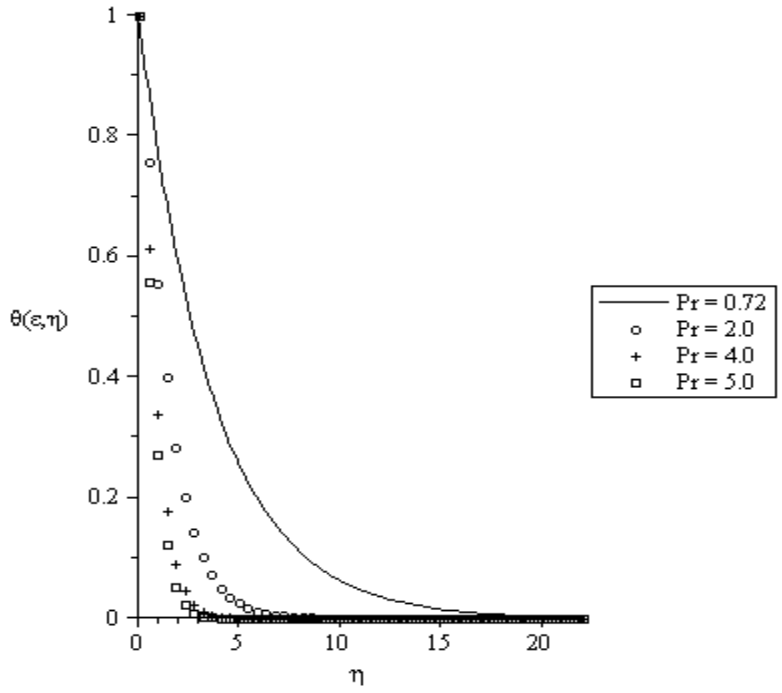

Figure 8: Temperature profiles for Ra = 1, M = 1, c = 0.5, ε = 1, λ = 0.5, Sc = 1, γ = 1.

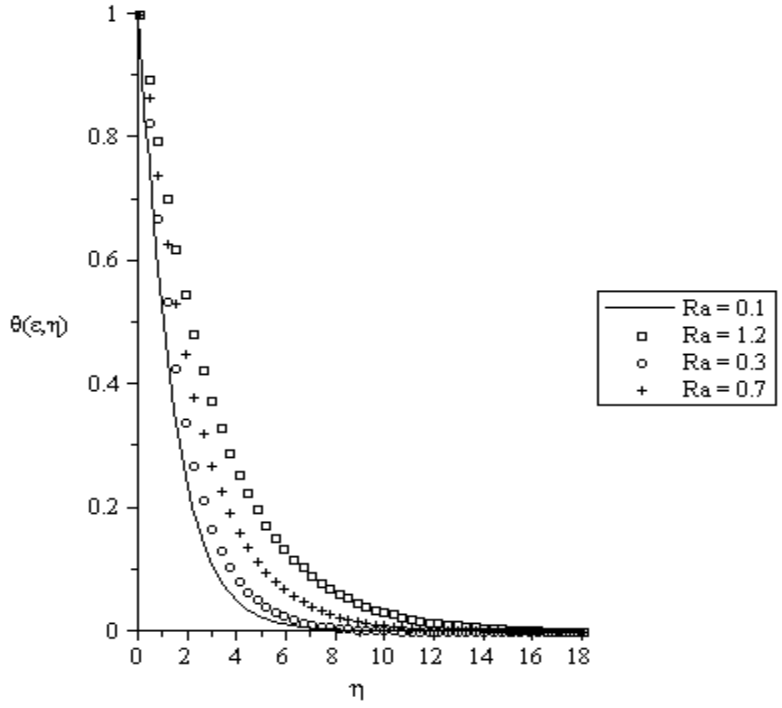

Figure 9: Temperature profiles for Pr = 1, M = 1, c = 0.5, ε = 1, λ = 0.5, Sc = 1, γ = 1.

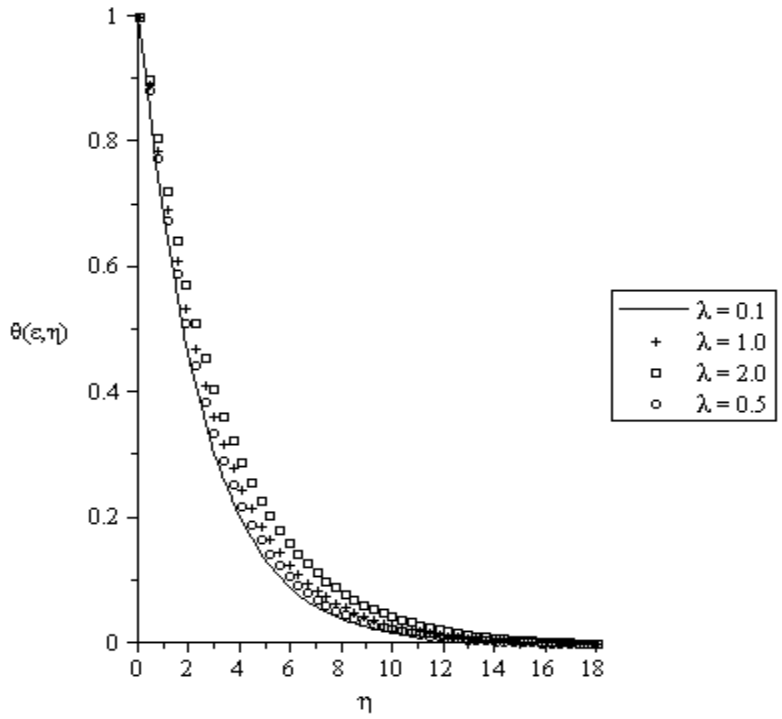

Figure 10: Temperature profiles for Pr = 1, M = 1, c = 0.5, ε = 1, Ra = 0.5, Sc = 1, γ = 1.

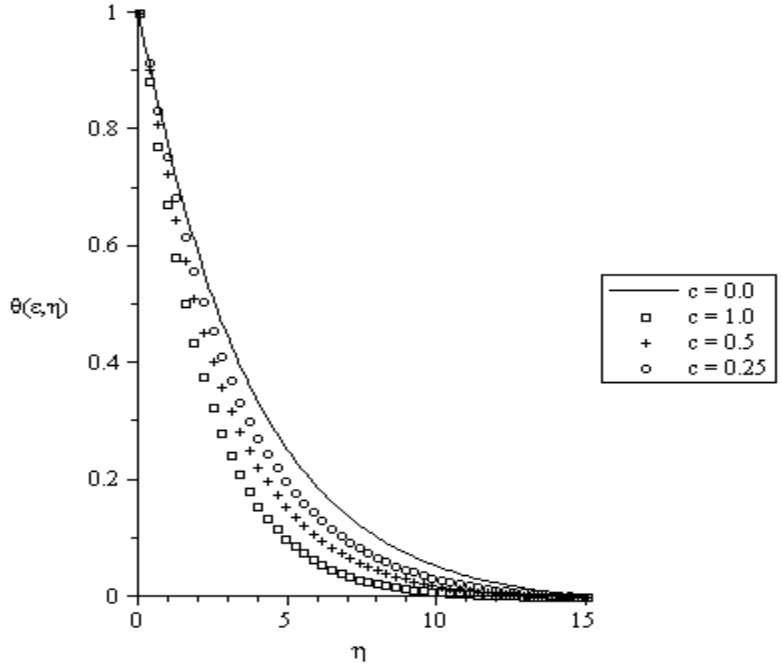

Figure 11: Temperature profiles for Pr = 1, M = 1, γ = 0.5, ε = 1, Ra = 0.5, Sc = 1, λ = 1.

C. Concentration Profiles

Figures 12–15 depict the fluid concentration profiles against spanwise coordinate η for varying values of physical parameters in the boundary layer. Figure 12 shows the influence of the magnetic field parameter M on the species concentration. Increasing the Hartman number increases the species concentration boundary layer thickness. Figure 13 described the influence of Schmidt number on the species concentration and it was observed that increase in Schmidt number leads to a decrease in the species concentration within the boundary layer due to the combined effects of buoyancy forces and species molecular diffusivity. Moreover, it is noteworthy that increasing values of chemical reaction parameter decreases the species concentration boundary layer thickness as illustrated in figure 14. Finally, it is noteworthy to note that increasing the ratio of stretching constant c decreases the species concentration boundary layer thickness across the plate.

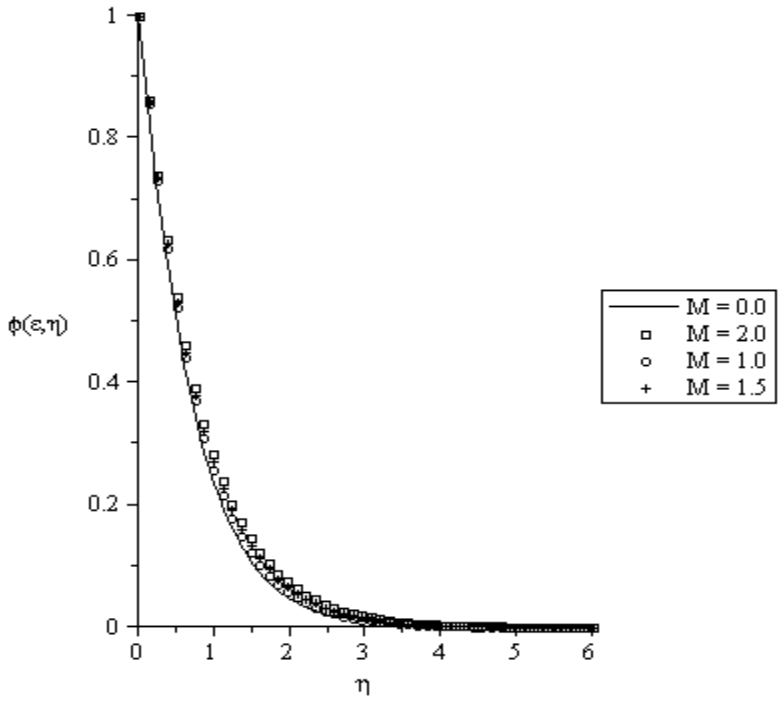

Figure 12: Concentration profiles for Ra = 1, Sc = 1, c = 0.5, ε = 1, λ = 0.5, Pr = 1, γ = 1.

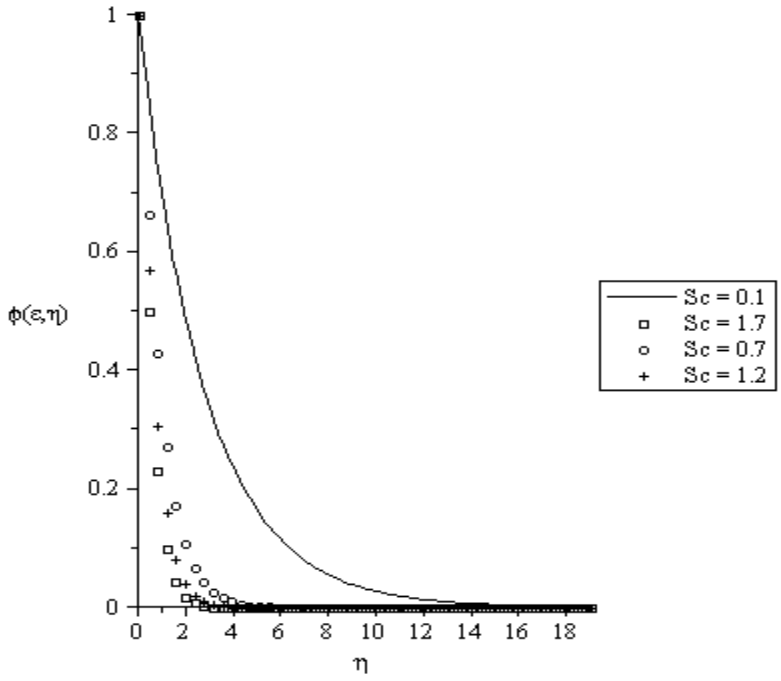

Figure 13: Concentration profile for Ra = 1, M = 1, c = 0.5, ε = 1, λ = 0.5, Pr = 1, γ = 1.

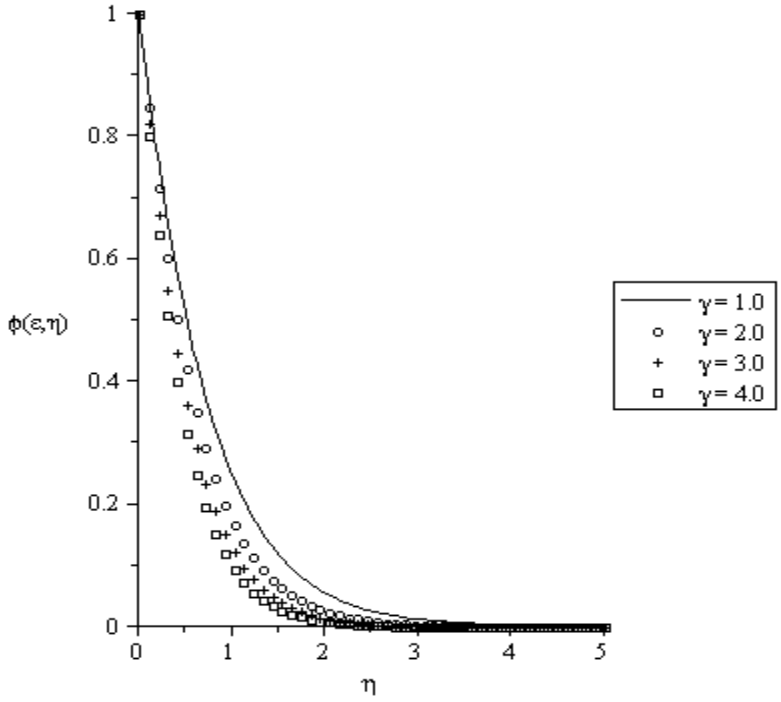

Figure 14: Concentration profiles for Pr = 1, M = 1, c = 0.5, ε = 1, Ra = 0.5, Sc = 1, λ = 1.

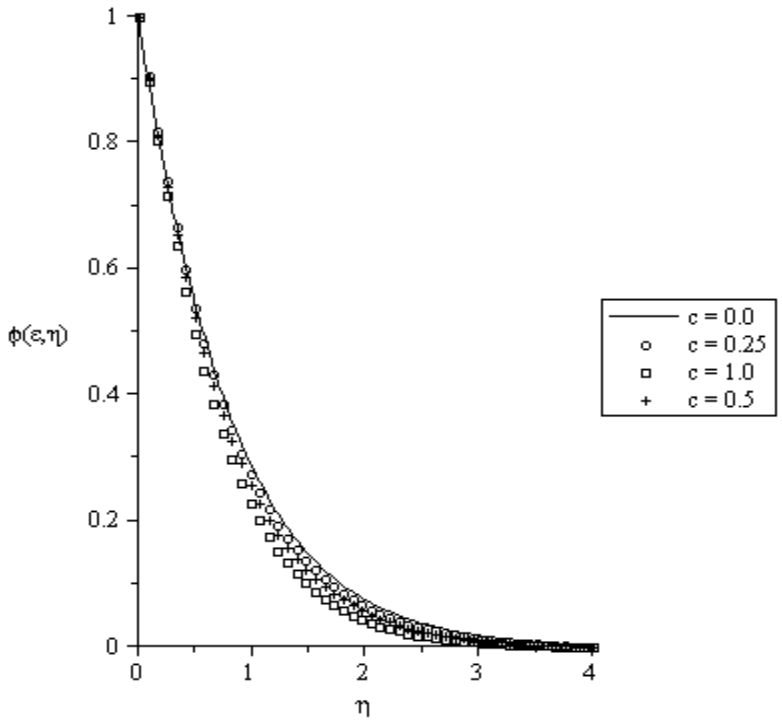

Figure 15: Concentration profiles for Pr = 1, M = 1, γ = 0.5, ε = 1, Ra = 0.5, Sc = 1, λ = 1.

5. Conclusions

This present article discusses a mathematical model for the transient flow with heat and mass transfer in the presence of thermal radiation. Three dimensional stretching case has been taken care off. Closed form solutions are first developed for ε = 0. For ε = 1, numerical solutions were obtained and interpreted for different involved parameters. The following conclusions were drawn as follows:

- The effects of Hartman number and the porosity parameter are qualitatively similar.
- The effect of decreasing values of M and λ is to increase the boundary layer thickness.
- The effects of Schmidt number is to decrease the concentration boundary layer thickness
- The effect of radiation parameter Ra is to increase the thermal boundary layer thickness through absorption.
- The thermal boundary layer thickness increases as Pr decreases.
- The influence of c and M on the skin friction coefficients are the same.
- The effect of the destructive chemical reaction parameter is to reduce the concentration field.
- The radiation parameter has no effect on the skin friction coefficients and the mass transfer rate.

Acknowledgements

POO wish to express his gratitude to Covenant University, Ota, West Africa for her generosity and support for this research work.

References

[1] Cortell R. Viscous flow and heat transfer over a nonlinearly stretching sheet. Appl Math Comput 184 (2007) 864–73.
[2] Cortell R. Flow and heat transfer of an electrically conducting fluid of second grade over a stretching sheet subject to suction and to a transverse magnetic field. Int J Heat Mass Transfer 49 (2006) 1851–1856.
[3] Liao SJ. Series solutions of unsteady boundary-layer flows over a stretching flat plate. Stud Appl Math 117 (2006) 2529–2539.
[4] Liao SJ. An analytical solution of unsteady boundary layer flows caused by an impulsively stretched plate. Commun Nonlinear Sci Numer Simulat 11 (2006)326–339.
[5] Ali ME, Magyari E. Unsteady fluid and heat flow induced by a submerged stretching surface while its steady motion is slowed down gradually. Int J Heat Mass Transfer 50 (2007) 188–195.
[6] Xu H. An explicit analytic solution for connective heat transfer in an electrically conducting fluid at stretching surface with uniform free stream. Int J Eng Sci 43 (2005) 859–874.
[7] Kumari M, Nath G. Analytical solution of unsteady three-dimensional MHD boundary layer flow and heat transfer due to impulsively stretched plane surface. Commun Nonlinear Sci Numer Simulat 14 (2009) 3339–3350.
[8] Hayat T, Abbas Z, Javed T. Mixed convection flow of a micro-polar fluid over a nonlinearly stretching sheet. Phys Lett A 372 (2008) 637–647.
[9] Sajid M, Hayat T. Influence of thermal radiation on the boundary layer flow due to an exponentially stretching sheet. Int Commn Heat Mass Transfer 35 (2008) 347–356.
[10] Sajid M, Hayat T, Pop I. Three-dimensional flow over a stretching surface in a viscoelastic fluid. Non-linear Anal: Real World Appl 9 (2008) 1811–1822.
[11] Xu H, Liao SJ, Pop I. Series solutions of unsteady three-dimensional MHD flow and heat transfer in the boundary layer over an impulsively stretching plate. Eur J Mech B 26 (2007) 15–27.
[12] Hayat T, Qasim M, Abbas Z. Homotopy solution for the unsteady three-dimensional MHD flow and mass transfer in a porous space. Commun Nonlinear Sci Numer Simulat 15 (2010) 2375-2387.
[13] England WC, Emery AF. Thermal radiation effects on laminar free convection boundary layer of an absorbing gas. J Heat Transfer 31 (1969) 37-44.
[14] Plumb OA, Huenfeld JS, Eschback EJ. The effect of cross flow and radiation on natural from vertical heated surfaces in saturated porous media. In: AIAA 16th Thermophysics conference, June 23-25/Palo Alto, Califonia, USA; 1981.
[15] Makinde OD, Olanrewaju PO, Charles WM. Unsteady convection with chemical reaction and radiative heat transfer past a flat porous moving through a binary mixture. Africa Matematika AM 1 (2011) 1-17.
[16] Makinde OD, Olanrewaju PO. Unsteady mixed convection with Soret and Dufour effects past a porous plate moving through a binary mixture of chemically reacting fluid. Chemical Engineering Communication (Accepted 2011)-In Press.
[17] Hayat T, Nawaz M, Sajid M, Asghar S. The effect of thermal radiation on the flow of a second grade fluid. Computers and Mathematics with Applications 58 (2009) 369-379.
[18] Hayat T, Abbas Z, Pop I, Asghar S. Effects of radiation and magnetic field on the mixed convection stagnation-point flow over a vertical stretching sheet in a porous medium. International Journal of Heat and Mass Transfer 53 (2010) 466-674.